Joint Centre for Mesoscale Meteorology, Reading, UK

A guide to aspects of water vapour imagery interpretation: the significance of dry regions

N. M. Roberts

Internal Report No. 109
NWP Technical Report No. 294

January 2000

Met Office Joint Centre for Mesoscale Meteorology Department of Meteorology
University of Reading PO Box 243 Reading RG6 6BB United Kingdom
Tel: +44 (0)118 931 8425 Fax: +44 (0)118 931 8791
www.metoffice.com

Designed and produced by the Met Office © Crown copyright 2001 01/0240 The Met Office logo is a registered trademark.

A guide to aspects of water vapour imagery interpretation: the significance of dry regions

Nigel M Roberts

JCMM, UK Met Office

January 2000

Contents

1.	**Introduction**	**2**
2.	**What does the water vapour channel show?**	**2**
2.1	Further aspects of water vapour imagery interpretation	3
3.	**The isolated PV anomaly, tropopause depression and 'dry eye'**	**5**
4.	**A baroclinic atmosphere - tropopause folding**	**6**
4.1	Deformation of the flow	7
4.2	Vertical motion	9
4.3	Tropopause folding	10
5.	**Water vapour imagery characteristics of vertical motion**	**12**
5.1	The dry eye dipole	12
5.2	Descent at trough base	12
5.3	Ascent and gradual shade transition	13
6.	**Potential instability**	**14**
7.	**Troughs, ridges and jet streaks**	**15**
8.	**Final comments**	**17**
9.	**References**	**18**

1. Introduction

Water vapour (WV) imagery provides us with dynamical insight into the upper troposphere. Of primary importance is the relationship between evolving patterns in the imagery and undulations in the height of the tropopause. Variations in tropopause height, inferred from the imagery, can be related to anomalies in potential vorticity (PV) (Mansfield 1996) from which aspects of the flow and temperature structure can be deduced (Hoskins et al 1985).

This report will discuss the relationship between patterns in WV imagery and key structures in flow, temperature and humidity. The focus is strongly on the dry (warm brightness temperature) regions in the imagery because it is these regions that are often associated with the initiation of strong convection and cyclogenesis. The relationship between WV imagery and thunderstorms is the subject of JCMM report 110 (Roberts 2000). A principle aim of this report is to provide a background for that discussion.

Section 2 of the report will present a basic overview of what the WV channel shows (based largely on the technical report by Weldon & Holmes 1991). Sections 3 to 7 will introduce some aspects of WV imagery interpretation that relate to key dynamical and thermodynamical structures in the upper troposphere and lower stratosphere. The information contained under each section will build on the previous one to develop an overall picture of the most important components. Section 8 has some brief final comments related to the use of WV imagery.

2. What does the water vapour channel show?

The satellite sensor measures radiation emitted by the earth's atmosphere at a wavelength centered around 6.7 microns. Radiation at this wavelength is strongly absorbed and re-radiated by water in the atmosphere. This means that the water content of the atmosphere determines how deep into the atmosphere the radiation received at the satellite comes from. If the atmosphere is moist then radiation received at the satellite is mostly from the top most layers because radiation from lower layers is absorbed and re-radiated by the moist layers above. If the atmosphere is dry then more radiation received at the satellite originates from lower layers because the dry layers above absorb it less.
The intensity of the radiation measured by the satellite can be converted into a 'brightness temperature'. Since the temperature of the troposphere generally decreases with height, the most intense radiation comes from lower levels where it has a warmer brightness temperature than radiation emitted from higher up. Therefore, a warmer brightness temperature indicates drier air and a colder brightness temperature indicates moister air. Figure 1 shows this in a schematic form.

Typically, the mid-latitude troposphere contains enough moisture at mid and upper levels to stop nearly all radiation from below around 700hPa reaching the satellite. Often the satellite will not 'see' much below 600hPa. Figure 2 shows weighting functions and brightness temperatures for radiation reaching the satellite for a single temperature profile with a variety of constant dew-point depressions. The percentage of total radiation reaching the satellite for a sounding with a 10°C dew-point depression is shown on the right hand side of Figure 2. In general, unless a column of air is very dry it is the layer between 200 and 600 hPa (lower stratosphere/upper troposphere) that contributes most to the radiation measured by the satellite. Where cloud is present only radiation above the cloud layer will reach the satellite unless the cloud is very thin and high.

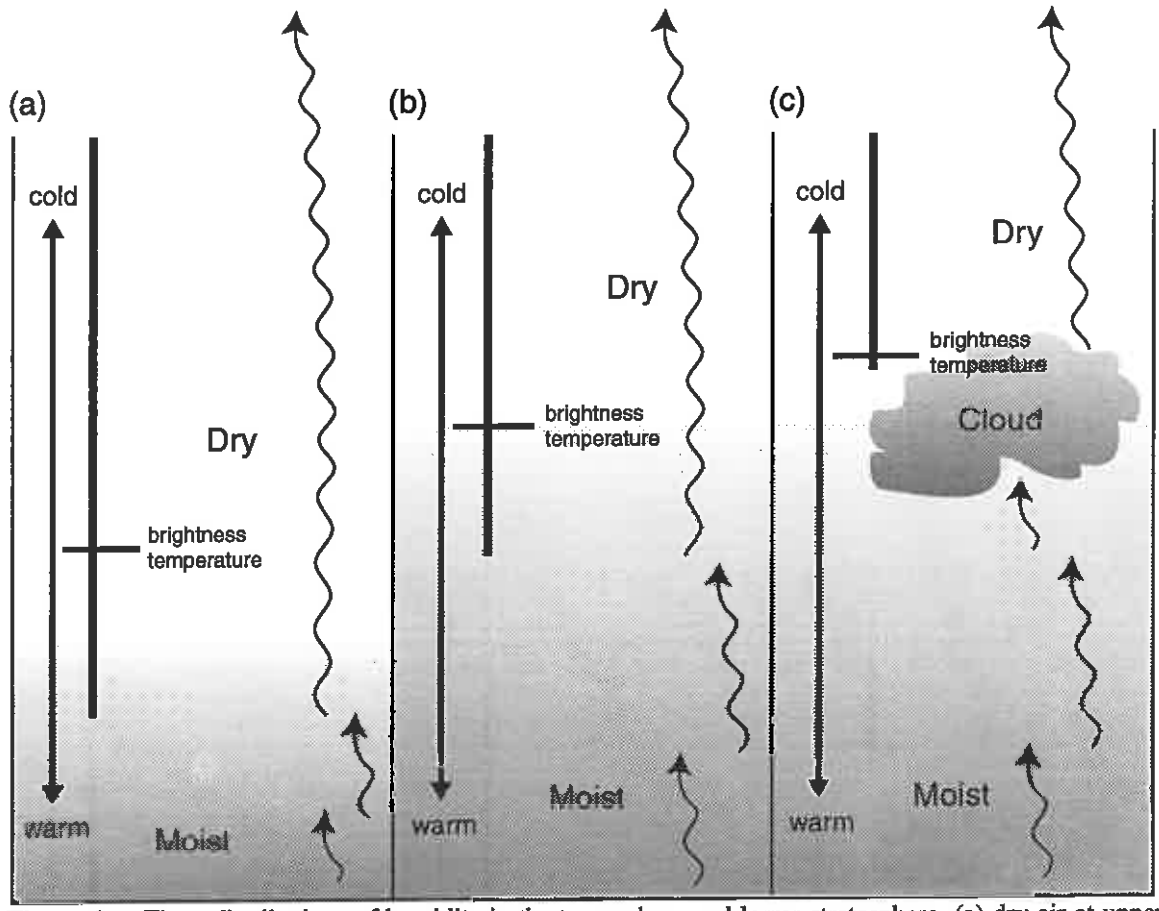

Figure 1. Three distributions of humidity in the troposphere and lower stratosphere. (a) dry air at upper and mid-levels with moist air at lower levels. (b) dry air at upper levels with moist air at lower levels and a transition zone between. (c) like (b) but with cloud at mid levels. Wavy lines with arrows represent upward radiation. The longest wavy lines represent the radiation received at the satellite originating from lowest down in the atmosphere. Broad dark lines to the left of each panel indicate the depth over which radiation received at the satellite originates. A schematic indication of brightness temperature from warm to cold is given in each panel showing a warmer brightness temperature for the drier column of air.

Moisture patterns in the upper troposphere/lower stratosphere can be examined by looking at images of water vapour channel brightness temperature which have been converted into a grey or colour scale. The convention used here is to show the dry regions (warmer brightness temperatures) in the blue/green colours or darker shades and the moist regions/cloud (colder brightness temperatures) in the red/yellow colours or lighter shades. Colour representation of WV imagery usually gives a clearer picture than grey scale.

2.1 Further aspects of water vapour imagery interpretation

There are other factors to take into account that can complicate the interpretation of water vapour imagery. The most important of these are briefly mentioned below.

(1) Seasonal variation

The mid-latitude troposphere in winter is colder and has a smaller height variation in temperature than in summer. In winter the air appears moister even if radiation reaches the satellite from lower levels because brightness temperatures are lower. The range of brightness temperatures is less in winter than summer. Dry regions can be more difficult to identify at high latitudes in winter.

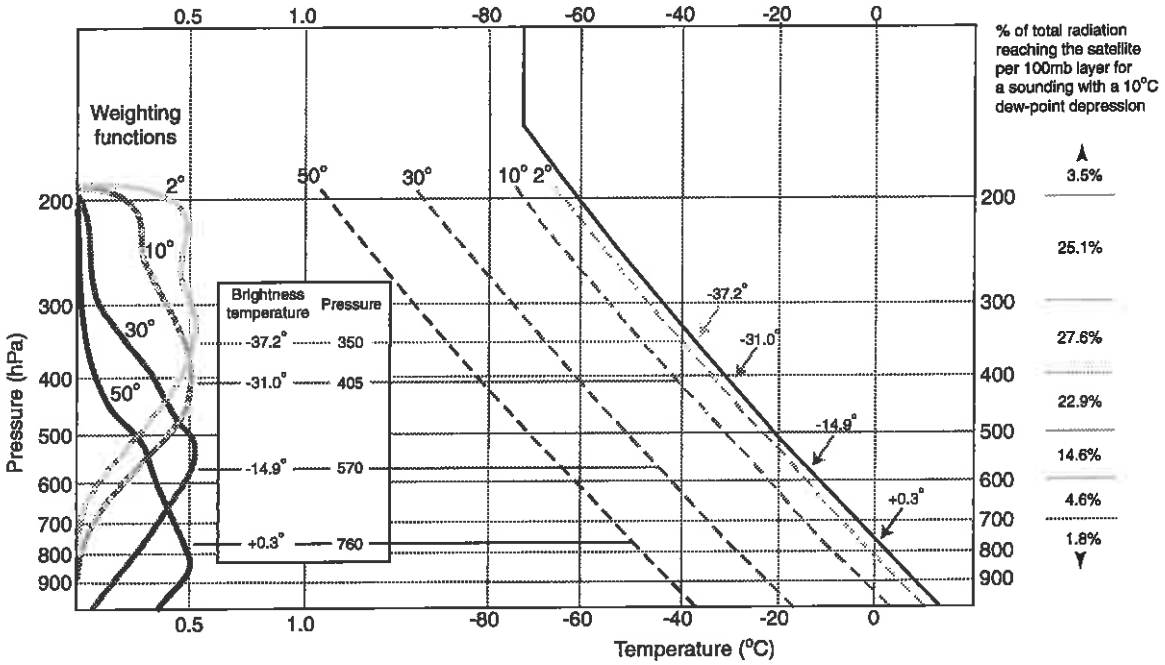

Figure 2. Weighting functions associated with different dew-point depressions for a single sounding. Taken from Weldon & Holmes 1991.

(2) Latitudinal variation

The troposphere gets colder and has a smaller height variation in temperature with increasing latitude. The air appears moister at higher latitudes because of lower brightness temperatures. The range of brightness temperatures is less at higher latitudes.

(3) Moisture banding

The brightness temperature of a column of atmosphere comprised of moist and dry layers is unlikely to be the same as the brightness temperature of a column of atmosphere with the same mean humidity but no layering. Since the mid-latitude troposphere often has moisture and cloud distributed in layers, it is important to be aware of the affect of such layering on the measured brightness temperature. Radiation emitted from a moist layer at the top of the troposphere is more likely to reach the satellite than radiation emitted from a lower layer; however it is also less intense than radiation emitted from a lower layer and therefore contributes less to the measured brightness temperature. This trade off between the intensity of the radiation and the likelihood of the radiation reaching the satellite is called the 'crossover effect' (Weldon & Holmes, 1991). The net result is that moist/cloud bands in the mid-troposphere contribute more to the measured radiation than moist/cloud bands in the upper or lower troposphere. A measurement of brightness temperature does not uniquely define the humidity profile of a column of atmosphere; many different distributions of humidity can give the same brightness temperature.

3. The isolated PV anomaly, tropopause depression and 'dry eye'

The tropopause marks the transition zone between dry stratospheric air and moister tropospheric air. In mid-latitudes the height of the tropopause above the ground generally decreases towards the poles, but also varies considerably as weather systems, troughs and ridges transport warm air to higher latitudes and cold air equatorwards. Typically, the height of the tropopause in mid latitudes varies between 6 and 12km, corresponding to the layer where water vapour imagery is most sensitive. Where the tropopause is low, a warmer brightness temperature is measured (dry region shaded blue in figures) because dry stratospheric air allows more radiation from lower levels to reach the satellite.

A good starting point towards understanding the relationship between the flow and temperature structure associated with variations in tropopause height, is to refer to an idealised model of an isolated tropopause depression (Thorpe 1985). Figure 3 shows this idealised lowering of the tropopause bringing dry stratospheric air with high potential vorticity (PV) down to lower levels. Consistent with this high PV anomaly is a cyclonic circulation and a bending of the isentropic surfaces in the troposphere upward towards the high PV anomaly. The consequence of the isentropic surfaces bending in such a way is to reduce the static stability of the troposphere below the tropopause depression. Essentially, a tropopause dip (or upper level positive PV anomaly) is associated with a cyclonic circulation and greater instability in the troposphere below. In more traditional terms this might be described as an upper-level trough and cold pool.

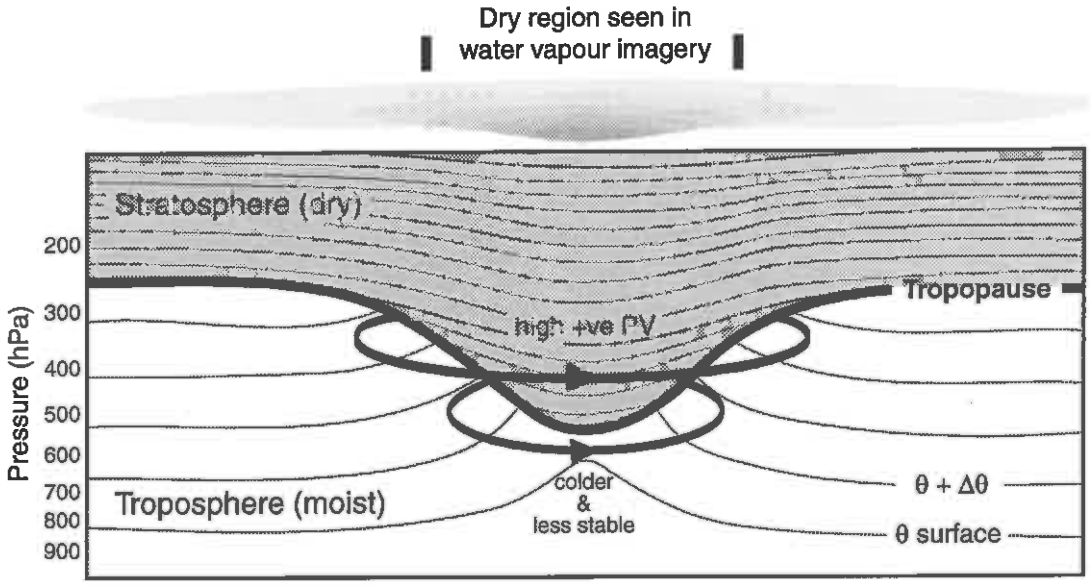

Figure 3. The 'dry eye'. (a) An idealised model of a tropopause depression based on calculations performed by Thorpe 1985. Thickest line shows the tropopause, thin lines show isentropic surfaces. The lines with the arrows indicate the vorticity associated with the tropopause depression.

If we were to observe such an isolated tropopause depression in WV imagery we would expect to see an almost circular area of warm brightness temperature as indicated in Figure 3. The question then is whether similar features are observed in the real atmosphere, and the answer is yes. In fact it is common to see circular or lens shaped dry regions in WV imagery ('dry eyes') on scales of a few tens to a several hundreds of kilometres. Observational studies of dry eye features have been

documented by Browning (1993) and Browning et al (1996). Figure 4 shows an example of just such a dry eye seen in WV imagery. Wind vectors at 500 hPa from a 3-hour forecast of the Met Office global model reveal the associated mid-tropospheric cyclonic circulation. In this case, the feature was well simulated by the model; this is not always so, particularly for smaller scale features.

If dry eye signatures in WV imagery are expected to be associated with cyclonic vorticity then they should show signs of rotation. Animation sequences on many occasions do show rotation in such features.

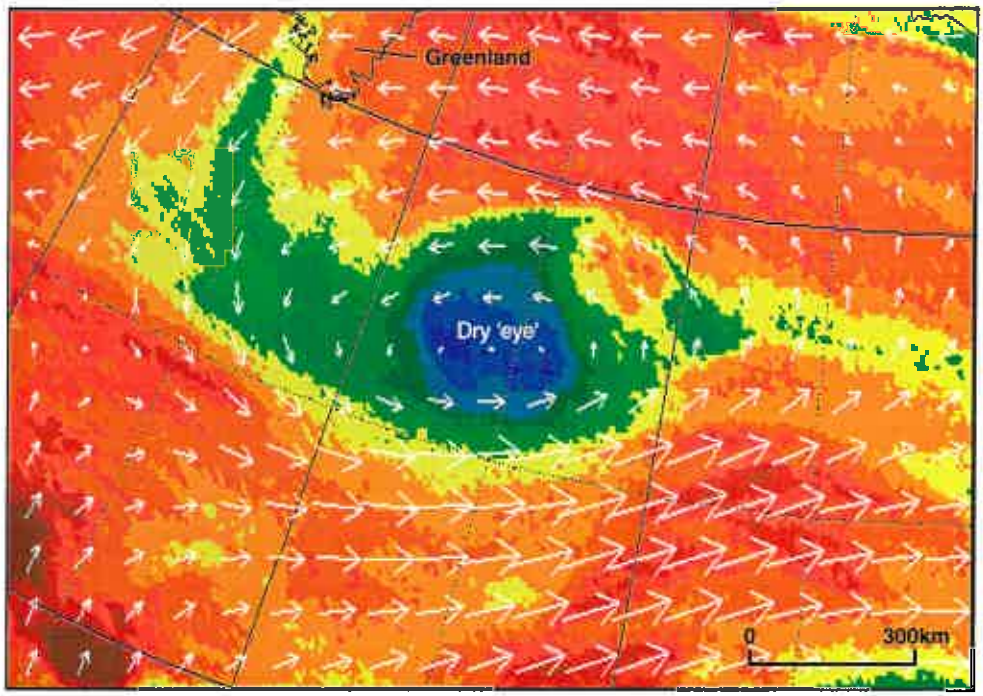

Figure 4. Meteosat WV image from 31/10/98 at 2130UTC. The dry air/warmest brightness temperatures are shown in the blue through green; the moist air or cloud/coldest brightness temperatures are shown in pink through orange. White arrows are wind vectors at 500hPa calculated relative to the velocity of the moving dry eye, from a good 3-hour forecast of the UK Met Office global model.

4. A baroclinic atmosphere - tropopause folding

The dry eye feature is a simple structure in a messy atmosphere. Assumptions have been made in relating an isolated tropopause lowering to what we see in WV imagery, these should to be mentioned.

Firstly, it was assumed that the stratosphere is dry and the troposphere is moist. Whilst this is generally true, it is not unreasonable to expect that some areas of the troposphere will by dry (Relative humidity < ~40%) and of course this will have an effect on the WV imagery brightness temperature. This can be an important consideration when using WV imagery. It especially has implications when comparing WV imagery with PV fields for PV modification (e.g. Dermitas & Thorpe 1997).

The second assumption was that the atmosphere is barotropic lower in the troposphere i.e. no horizontal temperature gradient, the isentropic surfaces are horizontal away from the tropopause depression (see Figure 3). In mid-latitudes there are horizontal temperature gradients and this also has implications for what we can deduce from WV imagery.

The characteristics of baroclinic regions that are important in WV imagery interpretation are now described.

4.1 Deformation of the flow

The shape of a tropopause depression is unlikely to be circular or lens shaped because of the stretching deformation of the flow associated with a developing baroclinic region. Figure 5 shows a schematic of the possible stretching effect on the shape of a dry eye approaching a strengthening baroclinic region if it is assumed that motion is adiabatic and the distortion is due to the larger scale flow pattern. This is the kind of configuration that might be expected at entrance region to a jet stream. Of course, the dry eye will have its own jet streak and thermal structure associated with it, so the situation is actually more complex. Figure 6 shows an example of a dry eye (the same as shown in Figure 3) becoming stretched along the thermal gradient as it moves southeast towards the UK.

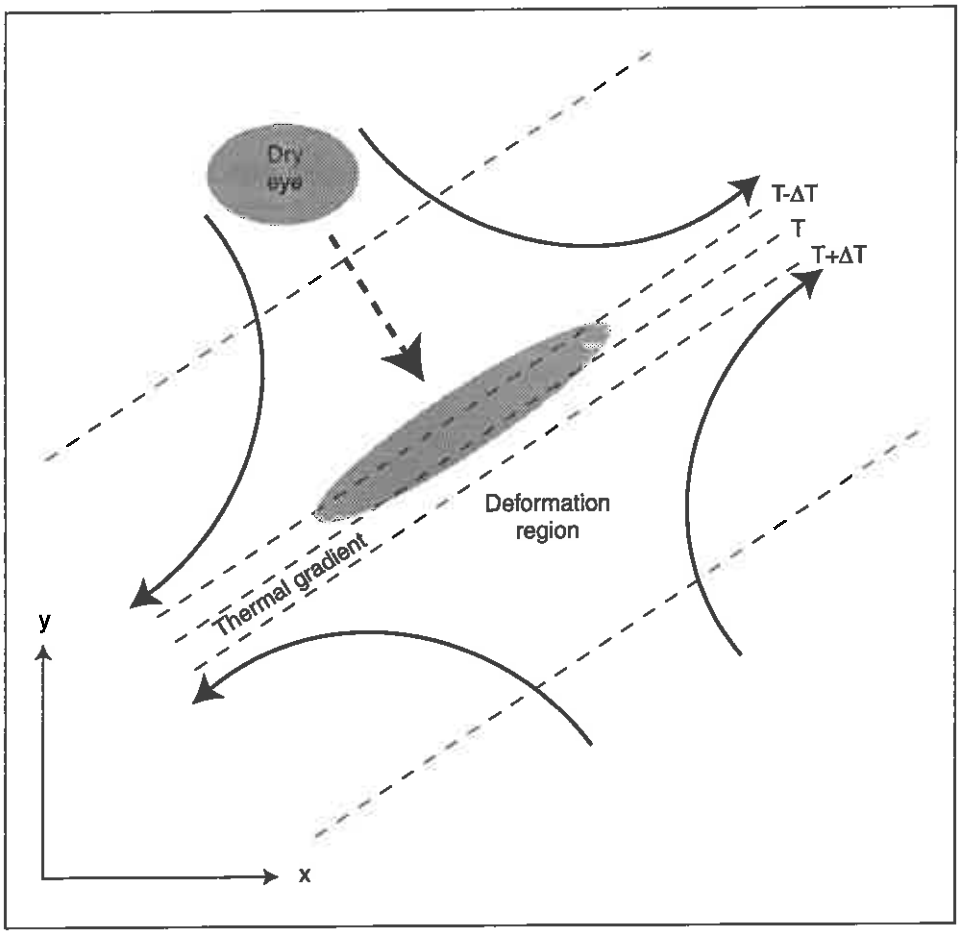

Figure 5. Schematic diagram of a dry eye becoming stretched in the vicinity of a large-scale deformation zone associated with a horizontal thermal gradient. Grey areas show a blue/dark/high radiance region in WV imagery. The thin dashed lines are isotherms. Continuous lines with arrows show the flow pattern. The thick dashed line indicates the movement of the grey area over time in this flow pattern.

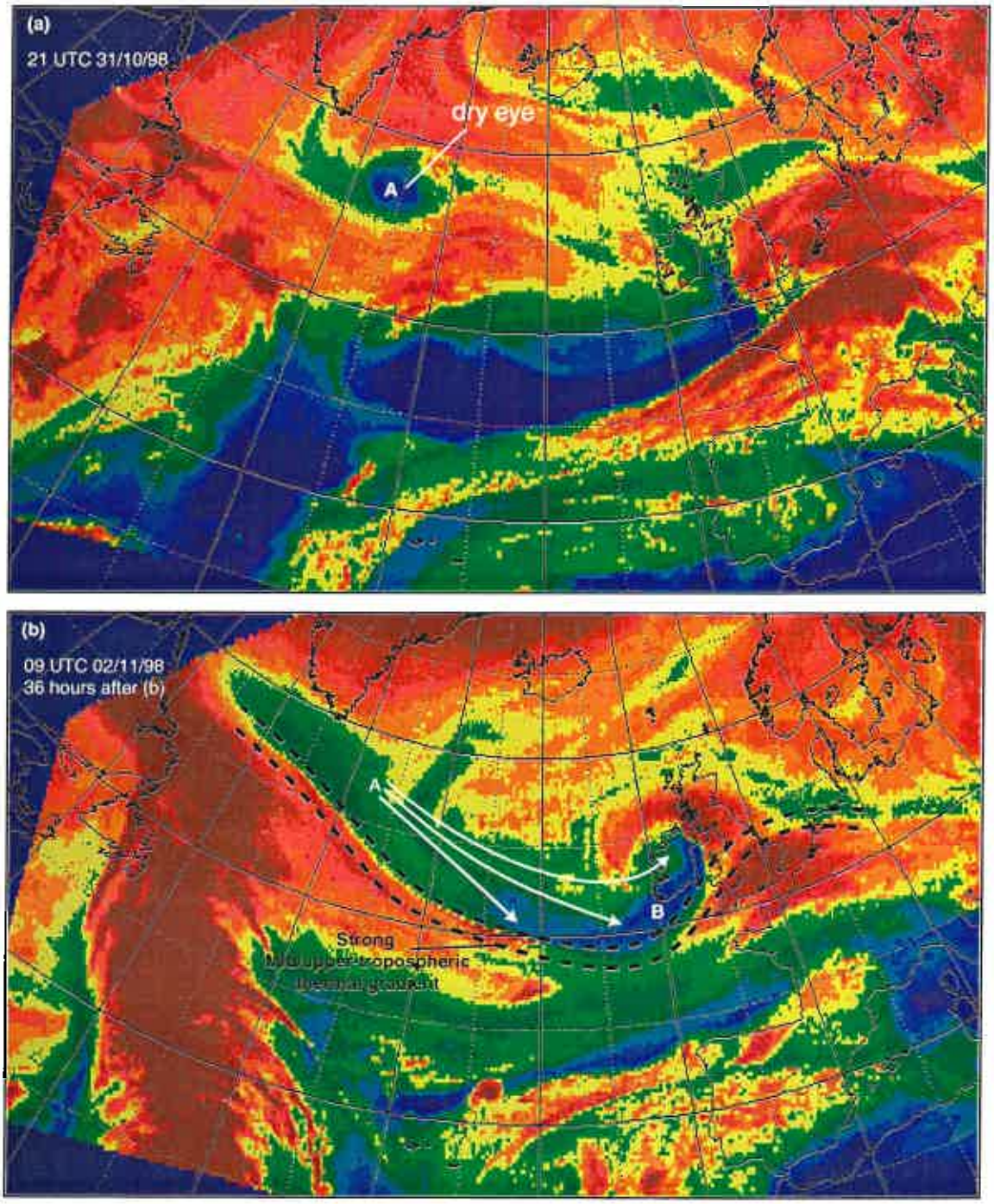

Figure 6. Meteosat WV images showing a dry eye feature 'A' becoming elongated in a baroclinic zone. Colours are as Figure 4. Dashed black lines in (b) show the axis of the jet stream. White arrows in (b) show how the dry eye has translated, enlarged and stretched between the two frames.

4.2 Vertical motion

The apparent stretching out of the dry eye in Figure 6 is not only a consequence of deformation of the background flow. Enlargement of the dry region is also enhanced by descent of air along sloping isentropic surfaces in the region of a horizontal temperature gradient. Air experiencing such adiabatic descent becomes warmer and drier (in the sense that the relative humidity decreases but the specific humidity remains the same). Recently descended upper/mid-tropospheric air appears drier (more blue) in WV imagery than before because radiation is now emitted at a warmer brightness temperature. It therefore becomes more problematic to exactly relate a dry region in WV imagery to a lowering of the tropopause, as some of the higher brightness temperature may be due to recently descended air below the dynamical tropopause. Nevertheless, the dynamic forcing for tropospheric air to descend also acts to lower the height of the tropopause; thus the kind of dry region shown in Figure 6(b) is still strongly associated with a tropopause depression or 'shelf' even though the relationship has become somewhat less clear. The picture of air-trajectories originating from a narrow source near the tropopause and fanning out into a wide convex pattern as they descend into the middle/lower troposphere has been described by Danielsen (1964) and is shown in Figure 7. Compare this with Figure 6. Wernli (1997) reinforced this idea by calculating trajectories from ECMWF analysis fields. He plotted clusters of coherent trajectories that descend more than 350hPa in a 48-hour period to reveal the same fanning out pattern.

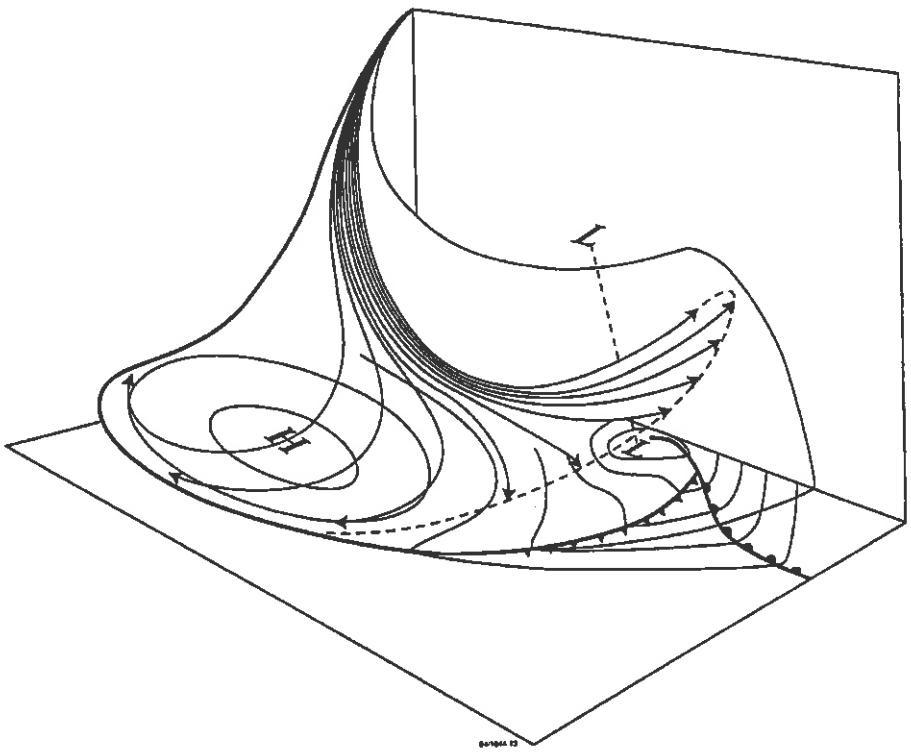

Figure 7. Trajectories of stratospheric (near tropopause level) air parcels on an isentropic surface descending and fanning out. The trajectories descend most in the anticyclonic region and re-ascend in the cyclonic region (Danielsen 1964).

4.3 Tropopause folding

As previously mentioned, air parcels that descend into the middle troposphere from the stratosphere or upper troposphere do so in a slantwise manner if the atmosphere is baroclinic. Such regions of descent are known as dry intrusions because the sheet of descending dry air intrudes into the troposphere at an angle and is sandwiched by moister air above and below. Descent of stratospheric air within a dry intrusion leads to a slantwise lowering of the tropopause, known as a tropopause fold (rather than a tropopause depression) because contours of PV become folded over in the vertical. A schematic diagram of a tropopause fold and WV image view of this fold is illustrated in Figure 8.

Care must be taken when interpreting WV imagery in the vicinity of tropopause folds. Much of the dry intrusion comprised of stratospheric air that has descended into the mid-troposphere is obscured from view by moister air above. A sharp boundary between moist and dry in the imagery is often an indication of an undercutting dry intrusion and upper-level jet streak associated with a baroclinic region. Figure 9(a) shows a dry region in WV image (on 17/02/97) with a sharp transition to moist/cloudy air to the southeast and a more gradual transition to the northwest. This is a typical example of a dry intrusion descending towards the southeast behind a cyclone and undercutting the moist/cloudy air on the warm side of the jet stream. A cross-section from the UKMO Unified Model (run at 12km horizontal resolution) through the dry intrusion (figure 9(b)) clearly shows a narrow tongue of dry air originating from the stratosphere and extending down to 800hPa with a slope of around 1/125.

Dry intrusions tilt downward towards the warm-air side of thermal gradients. They slope forwards ahead of cold upper-level troughs (high upper-level PV anomalies) and rearwards behind.

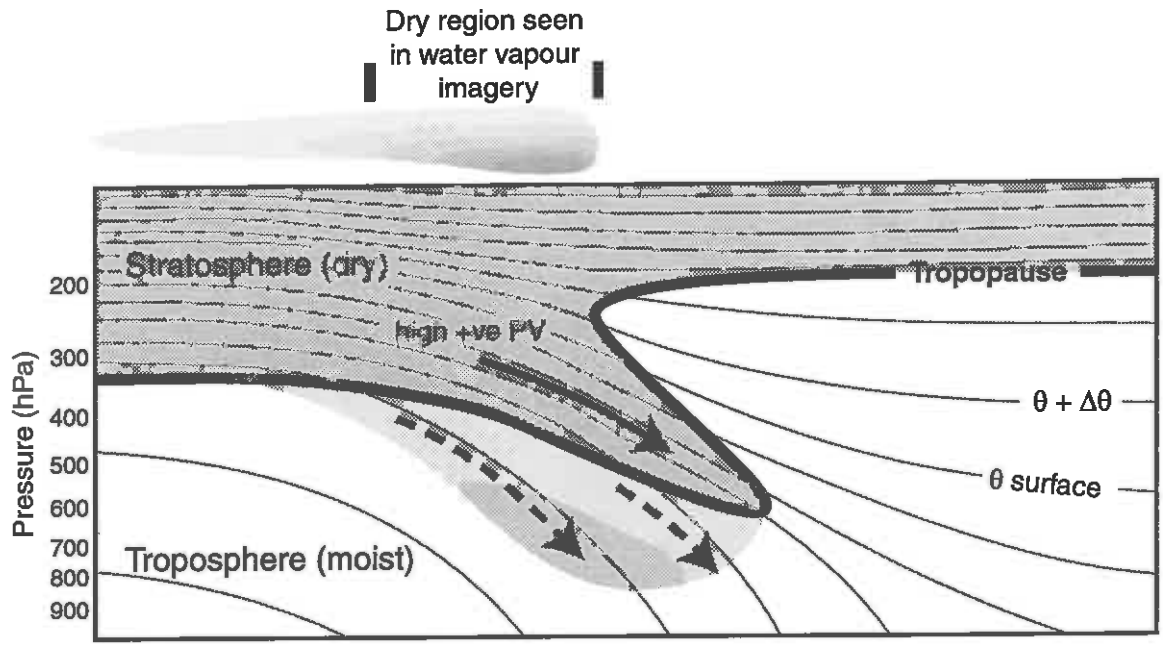

Figure 8. Schematic diagram of a tropopause fold. Thick line is the tropopause. Thin lines are isentropic surfaces. Continuous arrow shows stratospheric descent and dashed arrows show tropospheric descent.

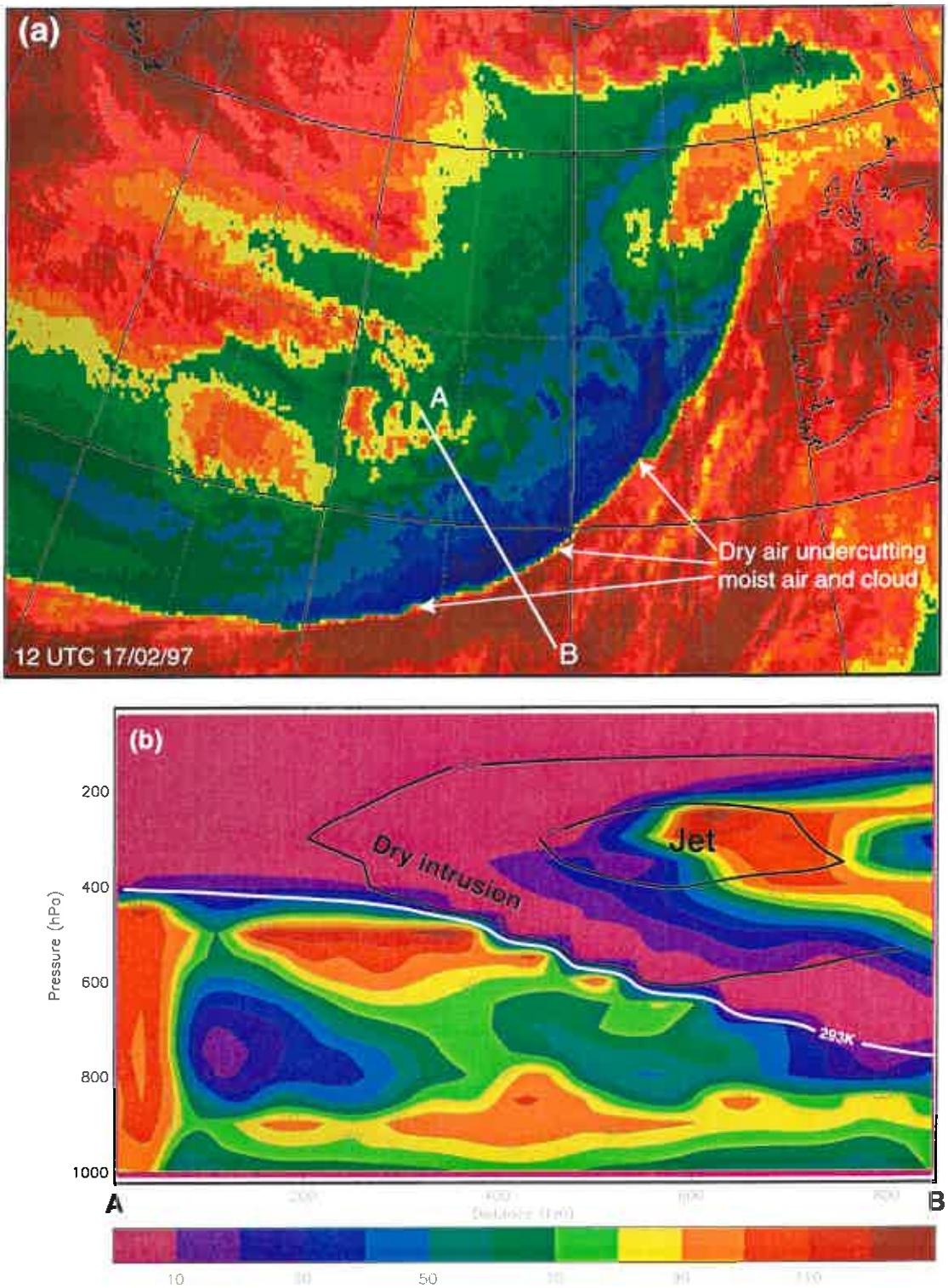

Figure 9. (a) Meteosat WV image using the same colour scheme as for Figure 3. (b) Cross section along the line AB in (a) from a UK Met Office Unified Model run at 12km horizontal resolution. Colours show relative humidity. Thick black lines show the 50 and 75m/s isotachs. The white line is the 293K isentropic surface. The stepped appearance at the base of the dry intrusion is largely a result of processing the model output at a vertical resolution of 50hPa.

5. Water vapour imagery characteristics of vertical motion

Vertical motion can have a significant effect on the appearance of WV imagery and is often a crucial factor in the conditions associated with the triggering of convection. Characteristic patterns in the imagery can be a good indicator of where the ascending or descending motion is occurring. The descent linked to flow along sloping isentropic surfaces in baroclinic regions has already been mentioned; now more specific phenomena are described in this light.

5.1 The dry eye dipole

In section 2.1 the flow and temperature structure associated with a stationary dry-eye feature was examined without considering any vertical motion. Since a dry eye in WV imagery can be interpreted as an upper-level PV anomaly, then according to Hoskins et al we can expect ascent ahead of and descent behind a moving dry eye. The vertical motion is largely associated with rearward flow relative to the moving upper-level PV anomaly along the bowed isentropic surfaces. This ascent ahead and descent behind dipole structure can also be seen in the forcing patterns for vertical motion from quasi-geostrophic theory (e.g. Clough et al 1996). As previously described, vertical motion can be diagnosed from changes in brightness temperature in WV imagery. A dry eye feature will have a tendency to become more blue (or darker in grey shades) in the region where descent is occurring, coupled with a tendency to become more red (or lighter) in the ascent region ahead (see Figure 10(a)). The ascent region becomes very apparent if the lifting is sufficient for clouds to form and more especially if convection is triggered. This is a favoured region for organised convection to occur and may lead to comma-cloud formation (again see Figure 10(a)) and sometimes cyclogenesis. A moving dry eye, especially if it is becoming more blue (darkening), can be a good indicator that convection will be triggered ahead of the dry eye later if conditions at lower levels are suitable.

5.2 Descent at trough base

Descending air at the base of extending upper troughs is revealed as an increasingly blue (darkening) region in WV imagery and such events are well documented by Weldon & Holmes. The darkest region is displaced from the upper-level PV maximum and occurs where the PV gradient is highly curved. The dipole ascent/descent structure still exists but on a larger scale with the ascending part being revealed by the polar front cloud band along the warm-conveyor belt ahead of the trough (Harrold 1973, Browning 1995). By it's very nature, a trough base darkening occurs in a baroclinic environment and the descent can be related to trajectories of air parcels descending from near tropopause level and eventually turning anticyclonically. This is equivalent to branch A in Figure 1 of Thorncroft et al (1993) or the anticyclonic trajectories in the picture by Danielsen (Figure 7). The schematic in Figure 10(b) shows the general appearance in grey shades of a 'typical' trough base dark region. Of course, troughs come along in a variety of shapes ranging from the large amplitude elongated sharp trough at one extreme to the small-scale small amplitude wave at the other that is actually best described as a dry eye feature. The importance of identifying blue/dark regions is that, whatever the trough pattern, they can be used to trace air that has descended while advecting from higher to lower latitudes. This air may later ascend in a return trip to higher latitudes and become involved in the triggering of convection.

5.3 Ascent and gradual shade transition

As shown schematically in Figure 10(c) a gradual transition from dark shades (greens/blues) to light shades (reds/yellows) along the direction of the system-relative mid/upper tropospheric flow is an indication of slantwise ascent. If the pattern is in a reasonably steady state then the gradual shade (colour) change is the result of a decrease in brightness temperature associated with adiabatic cooling. Usually, this pattern is observed when the flow is from lower to higher latitudes. Cloudiness may occur or convection break out where the air has experienced sufficient ascent

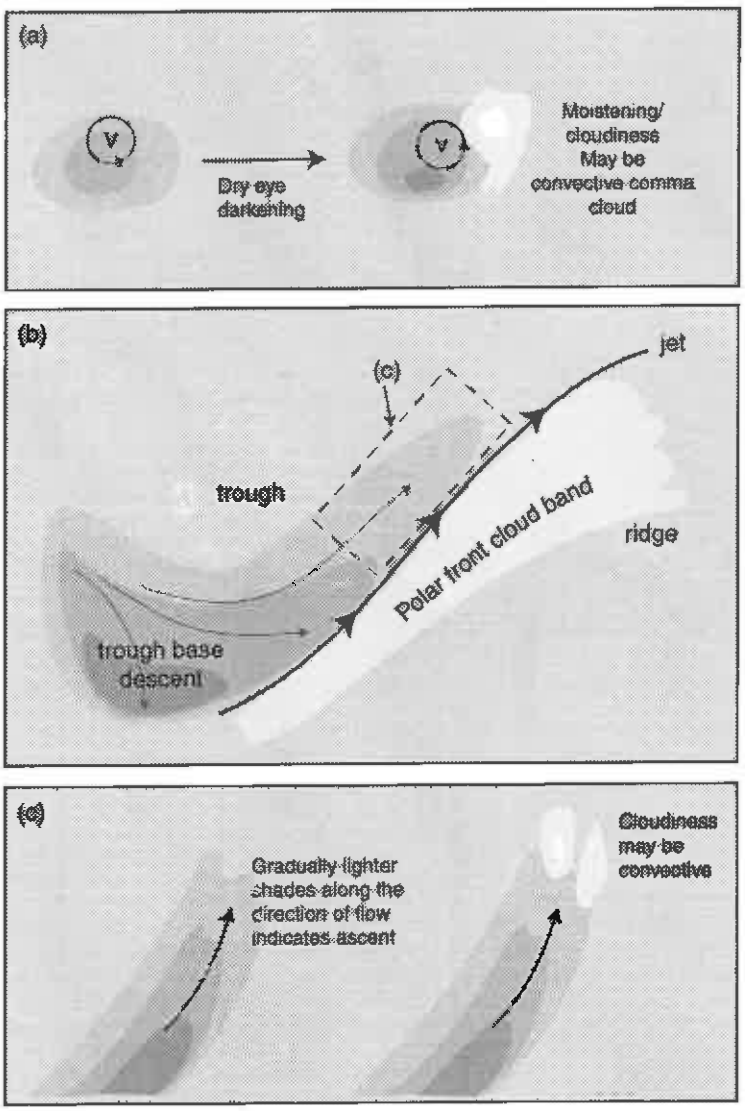

Figure 10. Schematic diagrams of the changing appearance of WV imagery associated with three patterns of vertical motion. Darker shades represent higher brightness temperatures and light shades represent cloud. (a) shows the darkening of a dry eye associated with a descent and vortex intensification along with the formation of convective cloud in the ascent region ahead of the dry eye. (b) shows a dark descending region at the base of an upper-level trough separated from the ascending polar front cloud band by an upper-level jet stream. (c) shows the gradual transition from darker to lighter shades along the direction of ascending flow (black arrows). Sufficient ascent may allow potential instability to be released and convective cloud to

develop (light shades). This region may be equivalent to the northern tip of the dark region indicated by the dashed box in (b).

6. Potential instability

A layer of the atmosphere is potentially unstable if the wet-bulb potential temperature (θ_w) decreases with height. It is possible for potential instability to be maintained if convection is prevented from occurring, either because there is insufficient moisture or because a more stable layer separates the high-θ_w air below from the low-θ_w air above. A typical situation where dry air in the troposphere is separated from the boundary layer by a stable layer might be found within an anticyclonic region characterised by mid-tropospheric descent. However, just because the air in a layer is drier than air in the layer below does not necessarily mean that there is potential instability. The required difference in θ_w can only arise if either the air in one layer has come from a different source region to the air in the other layer or the lower layer θ_w has increased due to surface heating and evaporation (neglecting radiative cooling).

WV imagery can be used to identify regions where the atmosphere is likely to be potentially unstable. Again, it is the characteristics of the blue/green (dark) areas in the imagery that are the focus of attention. These areas show where either the atmosphere has a locally lower tropopause or the upper/mid-troposphere is drier because of descent. Both of these factors are important. Firstly, if a column of air has a lower tropopause than its surroundings it is an indication that much of the air in the upper part of that column has come from higher latitudes. Dry regions can be traced back in the imagery to confirm this. Mid-tropospheric air that has arrived from higher latitudes will probably have a lower θ_w than the local surrounding air and more importantly the local boundary-layer air below. Secondly, the imagery highlights the regions where there has been mid/upper-tropospheric descent and therefore any potential instability generated by bringing air form higher to lower latitudes can be maintained by the formation of a more stable layer below the descent. The driest areas seen in the imagery are usually found in a region between the interior of an upper-level trough and the area of maximum tropospheric descent, so forming a crescent shape around the perimeter of the upper-level trough. This intermediate region is where the largest potential instability might be expected. Within the upper-level trough region the air may have a lower θ_w but has experienced less descent and is therefore too unstable for much of the potential instability to be maintained. Towards the greater descent region any potential instability can be maintained but the mid-tropospheric air may not have arrived from such high latitudes and therefore does not have such a low θ_w.

The reason that the amount of potential instability is so important is that it can determine the intensity of convection. The further equatorwards air can be transported without convection breaking out the more intense the convection is likely to be if it does eventually occur. Usually, the air has to re-ascend or the surface layer has to be sufficiently warm and moist before the stable layer can be 'broken down' and convection triggered. Ascent occurs when the flow turns cyclonically back towards higher latitudes. A typical pattern of interest in the imagery is a darkening dry zone associated with descent on the western and southern flank of an extending trough which can then trigger convection later on the eastern ascending side of the trough. Warm air advection at low levels ahead of the trough also acts to increase the likelihood of convective triggering.

Three reasons for caution when diagnosing regions of potential instability from WV imagery:

1) WV imagery can be a good guide to where potential instability may exist but it does not show the amount of potential instability.

2) Descent below around 600hPa is not usually seen in the imagery; the inference of descent below this level is necessary. It may be that at lower levels the region of potential instability is out of phase with the region expected from the imagery, particularly in highly baroclinic situations where advection is along sloping isentropic surfaces.

1) The amount of Convective Available Potential Energy (CAPE) through a column of the atmosphere is related more directly to the temperature lapse rate rather than the potential instability. The temperature lapse rate for any given potential temperature profile depends on recent history of the air in the column. Mid-level air transported from a dry plateau region (e.g. Spain) is likely to be well mixed and unstable compared to air transported from an oceanic warm-frontal region with the same mean θ_w. Despite this, potential instability is obviously still a necessary requirement for CAPE.

7. Troughs, ridges and jet streaks

This section looks at how the features in WV imagery examined so far, fit together into the larger scale pattern. Mid-latitude weather systems and larger-scale Rossby waves act to transport cold (warm) air, characterised by a low (high) tropopause, from higher (lower) to lower (higher) latitudes. WV imagery can be used to identify upper-level troughs and ridges associated with these waves, primarily because of the variation in the height of the tropopause. The best way of demonstrating this is to show a WV image as an example and pick out the salient features. This is done using Figure 11 as the example.

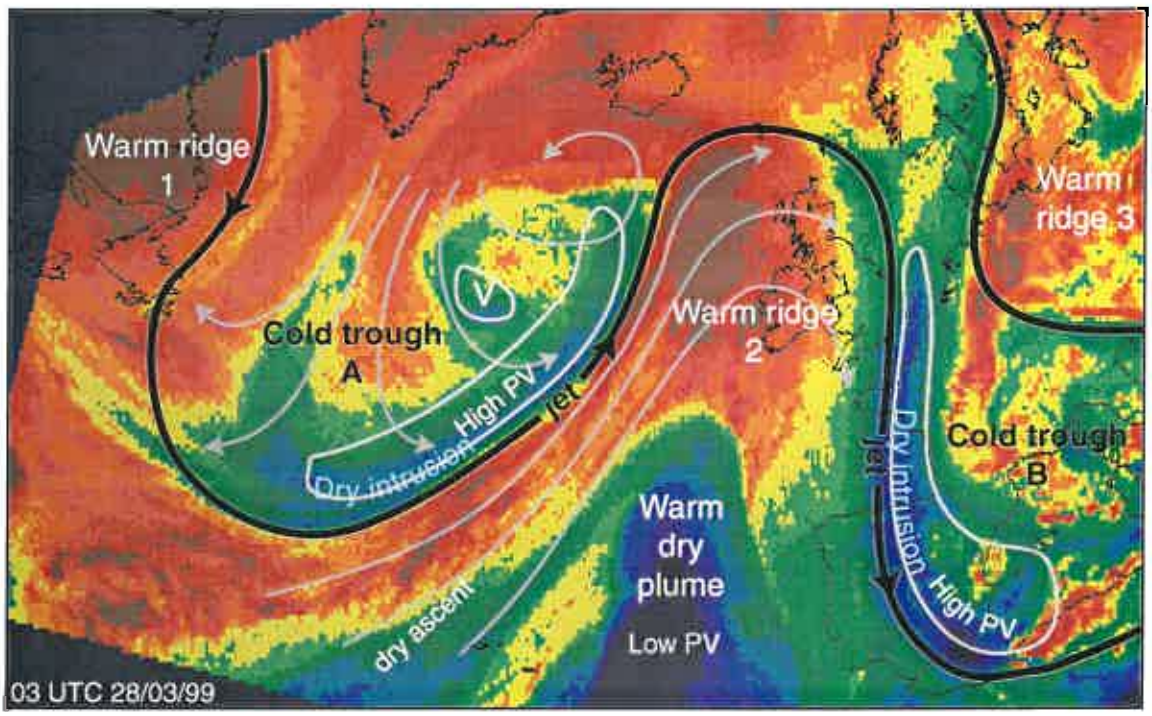

Figure 11. Meteosat WV image using the same colour scheme as Figure 3. The content is discussed in the text.

Two troughs (A & B) and three ridges (1,2 & 3) are labelled. The waving black line marks out these troughs and ridges by following the upper-level jet stream and thermal gradient. The

position of this line can be determined from the WV image, and although this requires experience in looking at these pictures, some of the features seen here are very similar to those shown in previous examples.

The forward edge of Cold Trough A is well defined by a dry intrusion undercutting the polar front cloud band in the warm air ahead. This dry intrusion, as in the example in section 2.3.3, is characterised by a strip of high upper-level PV (white line) associated with a lowering of the tropopause. The elongated nature of the high-PV strip is associated with a large-scale stretching of the flow and an intensified upper-level jet, which in turn is linked to ageostrophic circulations that lead to descent within the dry intrusion (Keyser & Shapiro 1985). A representation of the isentropic system-relative flow pattern within trough A and the warm conveyor belt is shown with the light-grey arrows. The jet stream is along the confluent asymptote of the relative flow pattern. The dry intrusion at the forward edge of trough A is an indication that the trough is propagating forwards (from west to east). The back edge of trough A is much less well defined, primarily because the air in that region is very cold so that dry air looks moist in the imagery and there is little distinction between dry and moist air.

The almost circular white ring marked with a V within trough A indicates a locally lower tropopause and high upper-tropospheric PV associated with a dry eye, much like the one already described in Figure 3. To the northeast of the dry eye is a yellow/orange region where convection has broken out ahead of the dry eye in the ascending part of the local ascent/descent dipole.

Trough B is well marked on its western flank by a dry intrusion associated with an upper-level high-PV anomaly. The dry region becomes darker towards the base of the trough where air-parcels have undergone the most descent. It is likely that the tropopause is folded on the western side of trough B and that the dark blue on this rearward part of the trough is an indication that the trough is not progressing forwards and may even be propagating backwards and extending. Convection has broken out widely within trough B as shown by the blobby red and yellow colours. The most intense convection (where the most lightning is detected) is occurring where the most potential instability is being released. This is occurring near the base of the trough at the forward edge of the high PV anomaly coincident with the eastern edge of the dry intrusion. Part of the western/northern edge of trough B is not well defined in WV imagery and here the black line is drawn on the basis of NWP fields primarily.

A striking feature within ridge 2 is the very blue area marked as a warm plume. It might be expected that this area, as with the other blue areas, highlights a region where the tropopause is lower - the opposite is true. As the label 'warm plume' suggests this is a region where the air is warm and probably of sub-tropical origin, so the satellite 'sees' warm brightness temperatures even from radiation received from high levels in the troposphere. This may cause confusion, but usually the signature of such features is quite distinctive. Occasionally, during a hot spell in summer, a warm plume advects northwards over Europe. If the northern fringe of this 'Saharan plume' shows a gradual transition from blues to yellow/red indicating ascent or the land surface is hot enough then scattered high cloud-base thunderstorms may break out. The area labelled 'dry ascent' is an example of a gradual change from south to north of blue to green indicative of slantwise ascent. The remaining area of ridge 2 is comprised of the polar-front cloud band to the east of the jet associated with an ascending moist warm conveyor belt.

8. Final comments

This report has described how WV imagery can be used to identify significant features in the flow, temperature and humidity patterns within the upper troposphere. In addition, it is possible to infer regions of mid-tropospheric ascent or descent and areas where the middle/lower-troposphere may be, or may become, potentially unstable. Much of this information is in cloud free areas where infrared or visible imagery is of little value. WV imagery provides a valuable analysis and forecast tool that should be utilised as much as possible.

A current established use for WV imagery is in the identification of analysis errors in NWP forecast models during cyclogenesis events. This is done in a subjective way by comparing PV or vorticity on an isentropic or pressure surface, in the vicinity of the jet stream, with the imagery (Mansfield 1997). Baroclinic wave cyclogenesis has been omitted as a topic in this report, despite its importance, because the determination of model error from WV imagery is often not straightforward in practice. Factors highlighted in this report such as tropopause folds, cloud, descent below the tropopause, the tilting of baroclinic structures along with an uncertainty in the height and depth of the layer the WV channel 'sees' all contribute to the difficulty in diagnosis.

A more simple approach may be to focus on smaller scale, more purely upper tropospheric and less baroclinic structures such as the 'dry eyes'. This has the advantage of making the interpretation much easier because the structures themselves are not as complex and the phase relationship with lower levels, so often a problem in baroclinic regions, is not so serious. These smaller-scale features can often be identified before cloud development and are important because they can be associated with significant weather events such as comma clouds and thunderstorms.

The relationship between patterns in WV imagery and thunderstorm development is presented in JCMM report 110.

9. References

Browning, K.A., 1993: Evolution of a mesoscale upper tropospheric vorticity maximum and comma cloud from a cloud-free two-dimensional potential vorticity anomaly. *Quart.J.Roy.Meteor.Soc.*, 119, 883-906

Browning, K.A., 1995: Mesoscale aspects of extratropical cyclones: an observational perspective. JCMM internal report, 44

Browning, K.A., N.M. Roberts and C.S.Sim, 1996: A mesoscale vortex diagnosed from combined satellite and model data. *Meteorol.Appl.*, 3, 1-4

Clough, S.A., C.S.A. Davitt, and A.J. Thorpe, 1996: Attribution concepts applied to the omega equation. *Quart.J.Roy.Meteor.Soc.*, 122, 1943-1962

Danielsen, E.F., 1964: Project Springfield Report. Defense Atomic Support Agency, Washington D.C. 20301 DASA 1517 (NTIS # AD-607980), 97 pp.

Dermitas, M. and A.J. Thorpe, 1997: Sensitivity of short-range weather forecasts to local potential vorticity modifications. JCMM internal report, 71

Harrold, T.W., 1973: Mechanisms influencing the distribution of Precipitation within baroclinic disturbances. *Quart.J.Roy.Meteor.Soc.*, 99, 232-251.

Hoskins, B.J., M.E. McIntyre and A.W. Robertson, 1985: On the use and significance of isentropic potential vorticity maps. *Quart.J.Roy.Meteor.Soc.*, 111, 877-946.

Keyser, D. and M.A. Shapiro, 1985: A Review of the Structure and Dynamics of Upper-Level Frontal Zones. *Mon.Wea.Rev.*, 114, 452-499.

Mansfield, D.A., 1996: The use of potential vorticity as an operational forecast tool. *Meteorol.Appl.* 3, 195-210.

Thorncroft, C.D., B.J. Hoskins and M.E. McIntyre, 1993: Two paradigms of baroclinic-wave life-cycle behaviour. *Quart.J.Roy.Meteor.Soc.*, 119, 17-55.

Thorpe, A.J., 1985: Diagnosis of balanced vortex structure using potential vorticity. *J.Atmos.Sci.*, 42, 397-406.

Weldon, R.B. and S.J. Holmes, 1991: Water vapour imagery: interpretation and Application to weather analysis and forecasting. NOAA *Technical Report*. NESDIS 57, National Oceanic and Atmospheric Administration, US Dept of Commerce, Washington DC, 213pp.

Wernli, H., 1997: A Lagrangian-based analysis of extratropical cyclones. II: A detailed case-study. *Quart.J.Roy.Meteor.Soc.*, 123, 1677-1706

CURRENT JCMM INTERNAL REPORTS

This series of JCMM Internal Reports, initiated in 1993, contains unpublished reports and also versions of articles submitted for publication. The complete set of Internal Reports is available from the National Meteorological Library on loan, if required.

1. **Research strategy and programme**
   K A Browning et al
   January 1993

2. **The GEWEX Cloud System Study (GCSS)**
   GEWEX Cloud System Science Team
   January 1993

3. **Evolution of a mesoscale upper tropospheric vorticity maximum and comma cloud from a cloud-free two dimensional potential vorticity anomaly**
   K A Browning
   January 1993

4. **The global energy and water cycle**
   K A Browning
   July 1993

5. **Structure of a midlatitude cyclone before occlusion**
   K A Browning and N Roberts
   July 1993

6. **Developments in systems and tools for weather forecasting**
   K A Browning and G Szejwach
   July 1993

7. **Diagnostic study of a narrow cold frontal rainband and severe winds associated with a stratospheric intrusion**
   K A Browning and R Reynolds
   August 1993

8. **Survey of perceived priority issues in the parametrizations of cloud-related processes in GCMs**
   K A Browning
   September 1993

9. **The effect of rain on longwave radiation**
   I Dharssi
   September 1993

10. **Cloud microphysical processes - a description of the parametrization used in the large eddy model**
    H Swann
    October 1993

11. **An appreciation of the meteorological research of Ernst Kleinschmidt**
    A J Thorpe
    May 1992

12. **Potential vorticity of flow along the Alps**
    A J Thorpe, H Volkert and Dietrich Heimann
    August 1992

13. **The representation of fronts**
    A J Thorpe
    January 1993

14. **A parametrization scheme for symmetric instability: test for an idealised flow**
C S Chan and A J Thorpe
February 1993

15. **The Fronts 92 Experiment: a Quicklook Atlas**
Edited by T D Hewson
November 1993

16. **Frontal wave stability during moist deformation frontogenesis**
Part 1: Linear wave dynamics
C H Bishop and A J Thorpe
May 1993

17. **Frontal wave stability during moist deformation frontogenesis**
Part 2. The suppression of non-linear wave development
C H Bishop and A J Thorpe
May 1993

18. **Gravity waves in sheared ducts**
S Monserrat and A J Thorpe
October 1993

19. **Potential vorticity and the electrostatics analogy: quasi-geostrophic theory**
C Bishop and A J Thorpe
November 1993

20. **Recent advances in the measurement of precipitation by radar**
A J Illingworth
April 1993

21. **Micro-physique et givrage: cloud microphysics and aircraft icing**
A J Illingworth
May 1993

22. **Differential phase measurements of precipitation**
M Blackman and A J Illingworth
May 1993

23. **Estimation of effective radius of cloud particles from the radar reflectivity**
N I Fox and A J Illingworth
May 1993

24. **A simple method of Dopplerising a pulsed magnetron radar**
A Hua, A J Illingworth and J Eastment
November 1993

25. **Radiation and polar lows**
George C Craig
February 1994

26. **Collected preprints submitted to the International Symposium on the Life Cycles of Extratropical Cyclones; Bergen, Norway, 27 June - 1 July 1994**
April 1994

27. **Convective frontogenesis**
Douglas J Parker and Alan J Thorpe
April 1994

28. **Improved measurement of the ice water content in cirrus using a total water evaporator**
Philip R A Brown and Peter N Francis
April 1994

29. **Mesoscale effects of a dry intrusion within a vigorous cyclone**
K A Browning and B W Golding
April 1994

30. **GEWEX Cloud System Study, Science Plan**
May 1994

31. **Parametrization of momentum transport by convectively generated gravity waves**
R Kershaw
May 1994

32. **Mesoscale Modelling Newsletter No 5**
May 1994

33. **Observations of the mesoscale sub-structure in the cold air of a developing frontal cyclone**
K A Browning, S A Clough, C S A Davitt, N M Roberts and T D Hewson
May 1994

34. **Longwave radiative forcing of a simulated tropical squall line**
Imtiaz Dharssi
July 1994

35. **On the nature of the convective circulation at a kata-cold front**
K A Browning
September 1994

36. **Collective preprints of papers submitted to the COST-75 International Seminar on Advanced Weather Radar Systems, Brussels, 20-23 September 1994**
November 1994

37. **Use of satellite imagery to diagnose events leading to frontal thunderstorms: Parts I and II of a case study**
K A Browning and N M Roberts
November 1994

38. **The role of spaceborne millimetre-wave radar in the global monitoring of ice cloud**
P R A Brown, A J Illingworth, A J Heymsfield, G M McFarquhar, K A Browning and M Gosset
December 1994

39. **Potential vorticity inversion**
Michal Ziemianski
October 1994

40. **Theory of mature tropical cyclones; a comparison between Kleinschmidt (1951) and Emanuel (1986)**
Suzanne L Gray
December 1994

41. **Dispersion and removal of pollutants during the passage of an atmospheric frontal system**
N R Gimson
December 1994

42. **The role of snow sublimation in frontogenesis**
D J Parker and A J Thorpe
December 1994

43. **Potential vorticity and the electrostatics Analogy: Ertel-Rossby formulation**
A J Thorpe and C H Bishop
December 1994

44. **Mesoscale aspect of extratropical cyclones: an observational perspective**
K A Browning
January 1995

45. **A polar low outbreak: evolution and mesoscale structures**
T D Hewson, G C Craig and C Claud
February 1995

46. **Generation of near-surface gusts of deep convection**
K Nakamura and R Kershaw
April 1995

47. **Attribution concepts applied to the Omega Equation**
S A Clough, C S A Davitt and A J Thorpe
June 1995

48. **Parametrization of mixed-phase cloud and precipitation**
Susan P Ballard and M Gerard Hutchinson
June 1995

49. **Short-range forecasting of stratocumulus: initialization prediction**
Susan P Ballard, Simon D Jackson and B Macpherson
June 1995

50. **Contributions of the JCMM/Dept of Meteorology Radar Group to the 27th AMS Radar Meteorology Conference, Vail October 1995**
June 1995

51. **Cold pools in shear**
Douglas J Parker
September 1995

52. **High-resolution analysis of frontal fracture**
K A Browning, S P Ballard and C S A Davitt
September 1995

53. **The albedo of broken cloud fields: calculations using a modified two stream radiation code**
Imtiaz Dharssi and Roy Kershaw
October 1995

54. **Parametrization of momentum transport by convection. I: theory and cloud modelling results**
R Kershaw and D Gregory
November 1995

55. **Variation of frontal structure along a cold front**
K A Browning and N M Roberts
November 1995

56. **Secondary frontal waves**
Douglas Parker
December 1995

57. **Objective fronts**
T D Hewson
March 1996

58. **Mesoscale analysis of the activation of a cold front during cyclogenesis**
K A Browning, N M Roberts and A J Illingworth
June 1996

59. **Investigation of different representations of rain in a 1-d evaporation model**
H Swann
May 1996

60. **Parametrization of diabatic processes in the inversion of the omega-equation**
M Athanassiadou and A J Thorpe
June 1996

61. **The role of the environmental flow in the development of secondary frontal cyclones**
I A Renfrew, A J Thorpe and A Joly
June 1996

62. **Consequences of the geostrophic momentum approximation on barotropic instability**
S Malardel, A J Thorpe and A Joly
June 1996

63. **Contributions to the AMS/RMS Conference on Mesoscale Processes**
Reading, 9-13 September 1996

64. **Vorticity and potential vorticity in stratified flows interacting with an isolated obstacle**
Jorge A Gutiérrez and A J Thorpe
September 1996

65. **Triple point development: two case studies**
Douglas Parker
September 1996

66. **Radar observations of wind-shear splitting within evolving atmospheric Kelvin-Helmholtz billows**
D Chapman and K A Browning
April 1997

67. **Cold frontal structure derived from radar wind profilers**
K A Browning, D Jerrett, J Nash, T Oakley and N M Roberts
May 1997

68. **The dry intrusion and its effect on the frontal, cloud and precipitation structure of extratropical cyclones**
K A Browning - Text of invited special lecture at the Spring Conference
of the Meteorological Society of Japan, University of Tsukuba, 22 May 1997

69. **Met. Office Unified Model data, diagnostics, graphics programs, and other observational data available from the JCMM through the aegis of the Universities Weather Research Network (UWERN).** (Plus supplement)
Peter Panagi and Ed Dicks
June 1997

70. **Contributions of the JCMM/Dept of Meteorology Radar Group to the 28th AMS Radar Meteorology Conference.** Austin, Texas
September 1997

71. **Sensitivity of short-range weather forecasts to local potential vorticity modifications**
Meral Demirtas and Alan Thorpe
July 1997

72. **Objective identification of frontal wave cyclones**
T D Hewson
August 1997

73. **Attribution and its application to mesoscale structure associated with tropopause folds**
A J Thorpe
September 1997

74. **The role of the environmental flow in the development of secondary frontal cyclones**
Ian A Renfrew, Alan J Thorpe and Craig H Bishop
September 1997

75. **Potential vorticity: a short history of its definitions and uses**
Alan J Thorpe and Hans Volkert
September 1997

76. **Superposing semi-geostrophic potential vorticity anomalies**
H R Birkett and A J Thorpe
September 1997

77. **Short period forecasting of catchment-scale precipitation.**
Part 1: the role of Numerical Weather Prediction
M A Pedder, M Haile and A J Thorpe
September 1997

78. **Verification of the tracking technique used in an experimental cloud motion wind inferring system**
Z Wang, K A Browning and G A Kelly
October 1997

79. **A preliminary study of Fourier series analysis for cloud tracking with GOES high temporal resolution images**
Z Wang
October 1997

80. **Analysis of an ex-tropical cyclone after reintensifying as a warm-core extratropical cyclone**
K A Browning, G Vaughan and P Panagi
November 1997

81. **A JCMM overview of FASTEX IOPs**
S A Clough, H W Lean, N M Roberts, H Birkett, J-P Chaboureau, R Dixon, M Griffiths, T D Hewson and A Montani
January 1998

82. **Programs for PV inversion and modification**
Meral Demirtas
December 1997

83. **Release of potential shearing instability in warm frontal zones**
D Chapman and K A Browning
February 1998

84. **The European Cloud-Resolving Modelling Programme (EUCREM)**
Summary Report from the coordinator
P W White
April 1998

85. **A frontal wave database**
T D Hewson
April 1998

86. **Layering observed in dropsoundings from IOP 1 of Fronts 92**
S A Clough
May 1998

87. **Use of wind-shear displays for Doppler radar data**
D Chapman and K A Browning
May 1998

88. **Radar estimates of rainfall rates at the ground in bright band and non-bright band events**
T J Smyth and A J Illingworth
June 1998

89. **Correction for attenuation of radar reflectivity using polarisation data**
T J Smyth and A J Illingworth
June 1998

90. **The effects of convection on chemical reactions and precipitation scavenging**
Neil R Gimson
July 1998

91. **How to use the display program DISP**
Nigel Roberts
August 1998

92. **Conceptual models of cyclogenesis**
Adrian T Semple
August 1998

93. **Observations of oblate hail using dual polarisation radar and implications for hail detection schemes**
T J Smyth, T M Blackman and A J Illingworth
September 1998

94. **The semigeostrophic diagnosis of vertical motion. Part I: Formulation and co-ordinate transformations**
Mike A Pedder and Alan J Thorpe
September 1998

95. **The semigeostrophic diagnosis of vertical motion. Part II: Results for an idealised baroclinic wave life cycle**
Alan J Thorpe and Mike A Pedder
September 1998

96. **Convective destabilisation by a tropopause fold diagnosed using potential vorticity inversion**
Morwenna Griffiths, Alan Thorpe and Keith Browning
October 1998

97. **Forecast skill of the ECMWF model using targeted observations during FASTEX**
A Montani, A J Thorpe, R Buizza and P Unden
October 1998

98. **Observations and model simulations of the FASTEX IOP 16 frontal wave - effects of sublimation**
Sid A Clough, Humphrey W Lean, Nigel M Roberts and Richard M Forbes
December 1998

99. **The application of conceptual models in NWP**
Adrian T Semple
January 1999

100. **Mesoscale analysis of arc rainbands in a dry slot**
K A Browning and N M Roberts
January 1999

101. **Interaction of mesoscale tropopause depressions with a warm-core cyclone: observational and model analyses, and sensitivity to analysis errors**
K A Browning, A J Thorpe, A Montani, D Parsons, M Griffiths, P Panagi and E M Dicks
February 1999

102. **The use of water vapour imagery and PV inversion to adjust initial conditions in NWP**
Sean J Swarbrick
February 1999
This report is no longer available; see Internal Report No.108

103. **Summary notes for a lecture course on Waves in the Atmosphere and Ocean**
A A White
March 1999

104. **Results of a questionnaire on the operational value of conceptual models (CMs) of fronts and cyclones**
N M Roberts & M V Young
July 1999

105. **Contributions to the Poster Session at the 1998 UWERN Annual Science Meeting**
assembled by A A White
August 1999

106. **The objective analysis of dropsonde data from FASTEX**
Richard Forbes, Sid Clough, Mark Dixon, Andy Macallan & Nigel Roberts
January 2000

107. *NWP Technical Report No.302*
Implications for Mesoscale Modelling from a Study of the FASTEX IOP 16 Mid-latitude Cyclone
Richard M Forbes, Humphrey W Lean, Nigel M Roberts and Peter A Clark
March 2000

108. *NWP Technical Report No.291*
The use of water vapour imagery and PV inversion to adjust initial conditions in NWP
Final Project Report
Sean J Swarbrick
September 1999

109. *NWP Technical Report No.294*
A guide to aspects of water vapour imagery interpretation: the significance of dry regions
Nigel M Roberts
January 2000

Met Office Joint Centre for Mesoscale Meteorology Department of Meteorology
University of Reading PO Box 243 Reading RG6 6BB United Kingdom
Tel: +44 (0)118 931 8425 Fax: +44 (0)118 931 8791
www.metoffice.com